

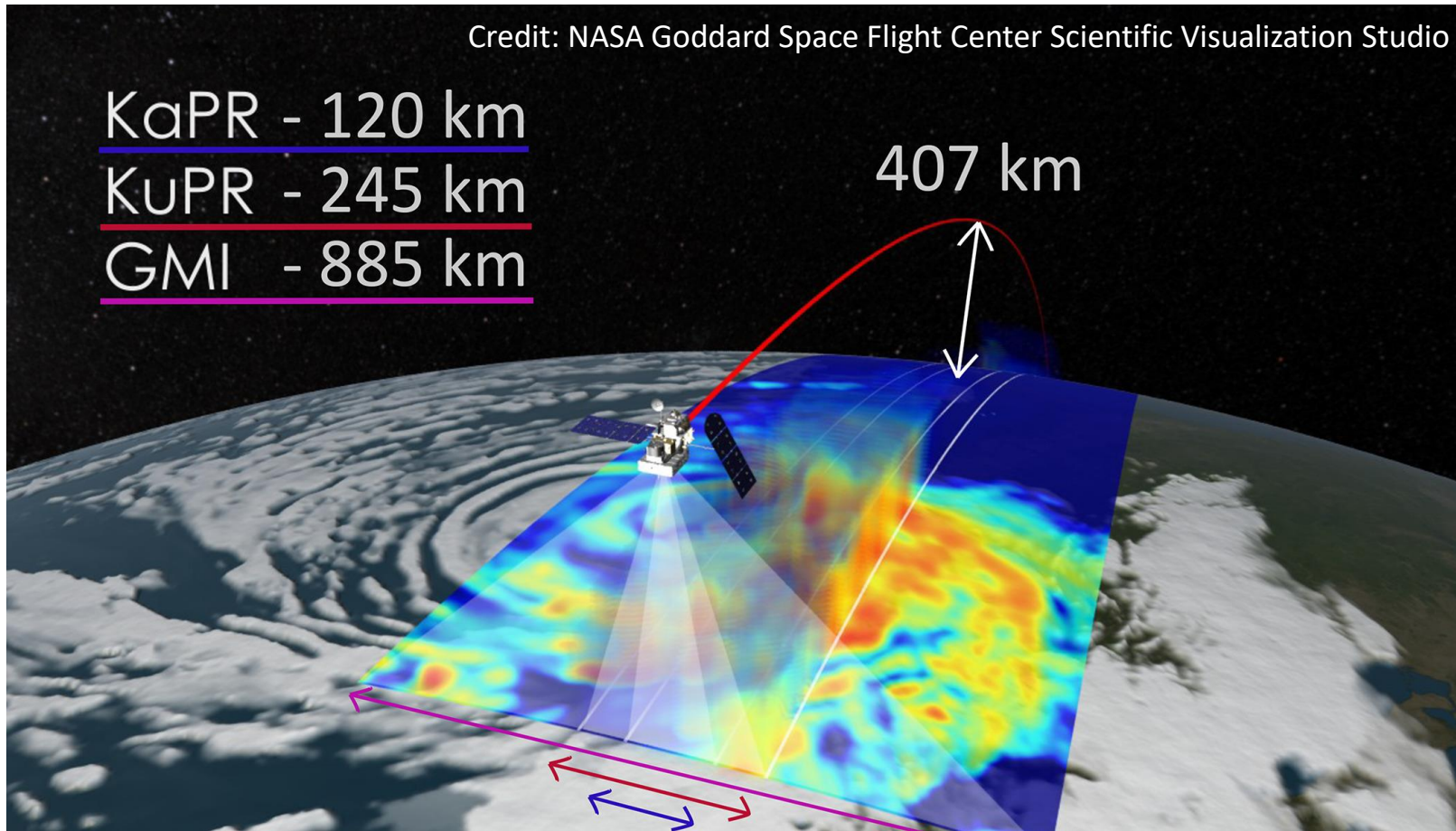
Credit: NASA Goddard Space Flight Center Scientific Visualization Studio

KaPR - 120 km

KuPR - 245 km

GMI - 885 km

407 km



The GPM-CO measuring over a mid-latitude storm.

GPHS-426

Climatology and *Remote Sensing*

RS Lecture 4

18 January 2024

Remote Sensing (4 X 2-hour classes)

Lecturer: Yizhe Zhan

- Principles of satellite remote sensing (Wed 13 Dec 2023)
- Meteorological satellites (Tues 19 Dec 2023)
- Passive remote sensing instruments (Thurs 11 Jan 2024)
- **Active remote sensing instruments (Thurs 18 Jan 2024)**

For course material and hands-on session,



https://github.com/yzhan-met/GPHS-426_RS.git

For reach out for questions, my EDU email is yizhe@illinois.edu.

Outline

1. Active sensing instruments and products

Scatterometer

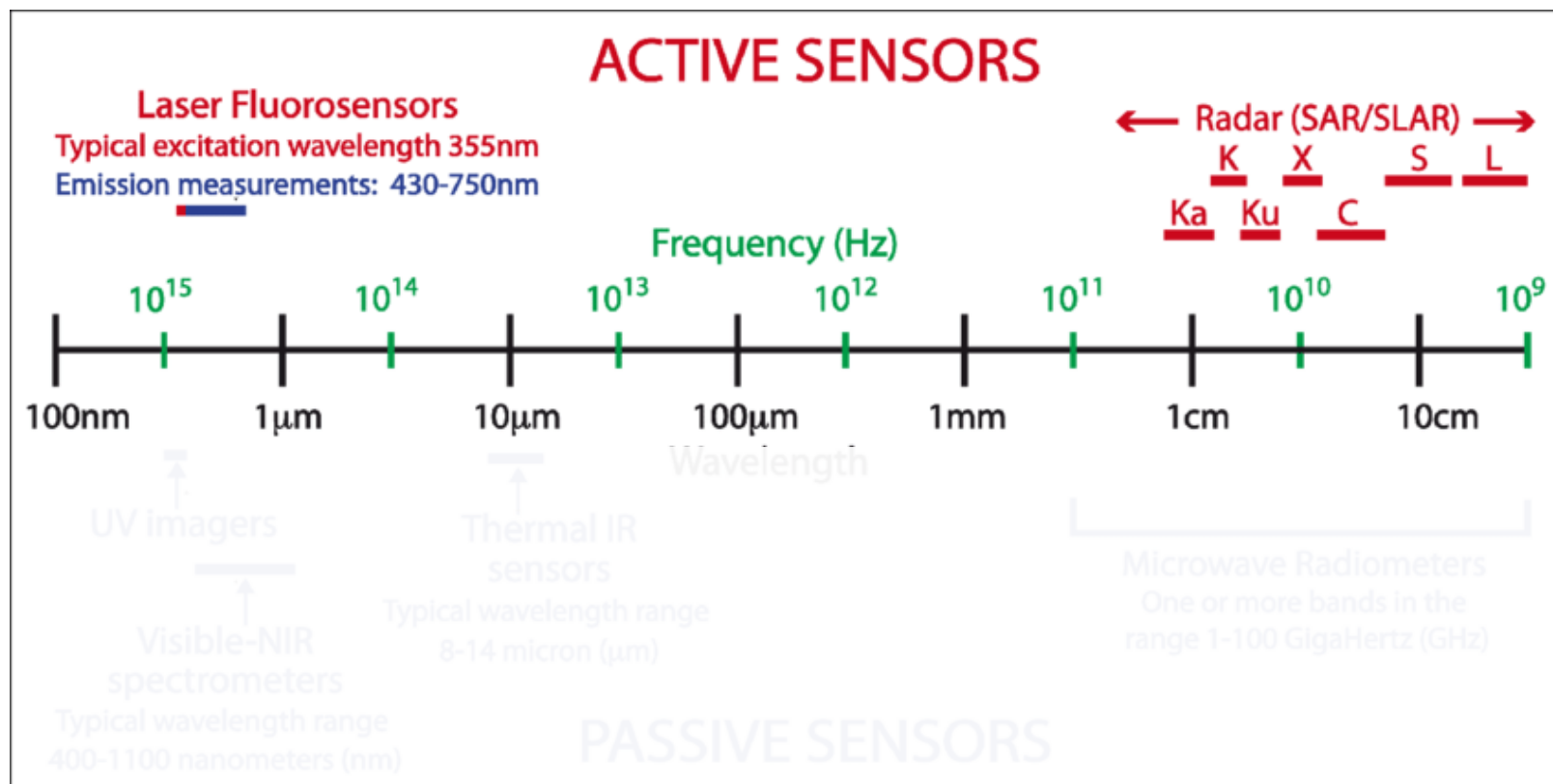
- Example instrument: ASCAT
- Example product: SSW

GNSS Radio Occultation

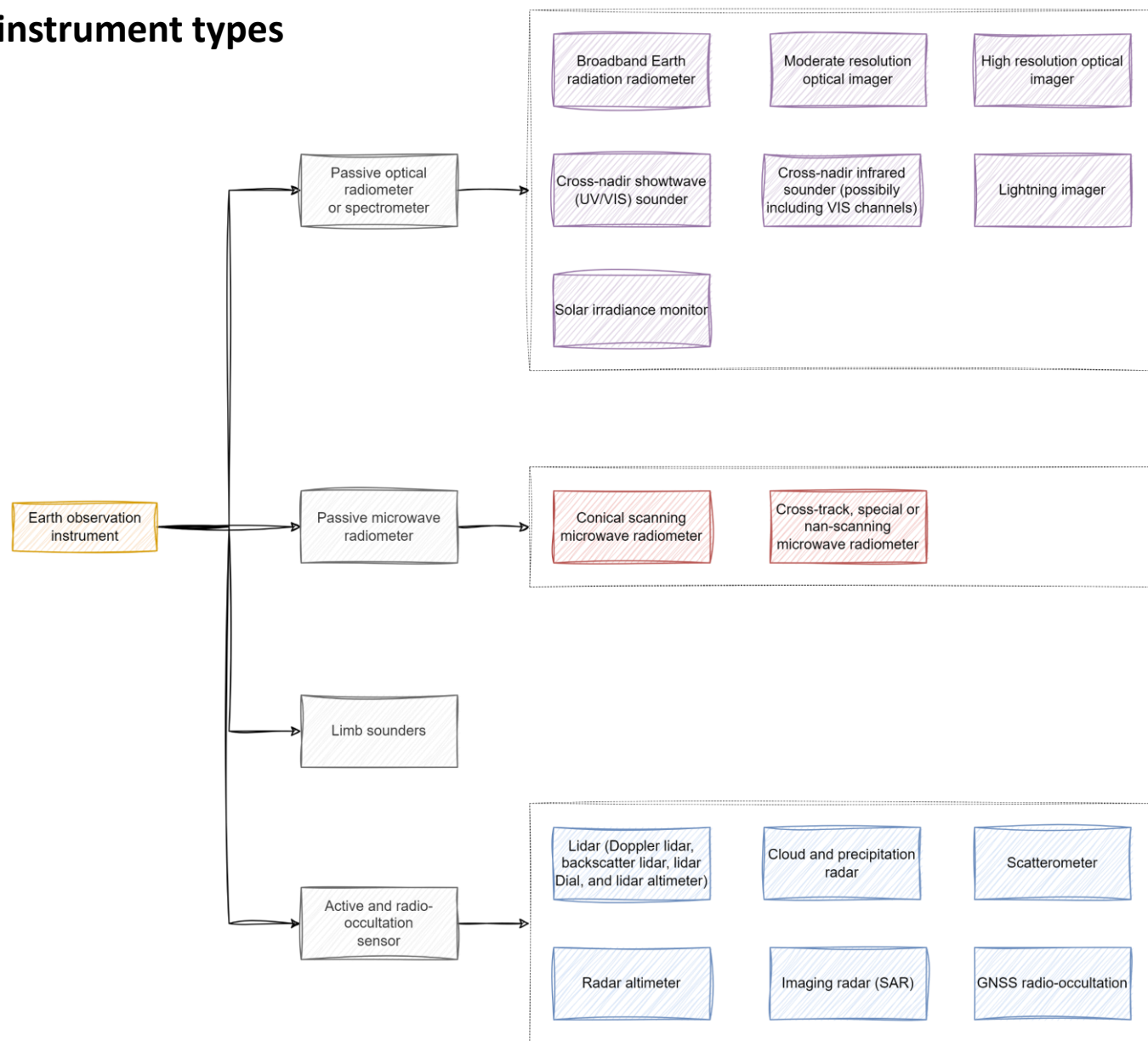
- Example instrument: TGRS
- Example product: temperature sounding

2. Future satellite programs

Remote sensing instruments (sensors)

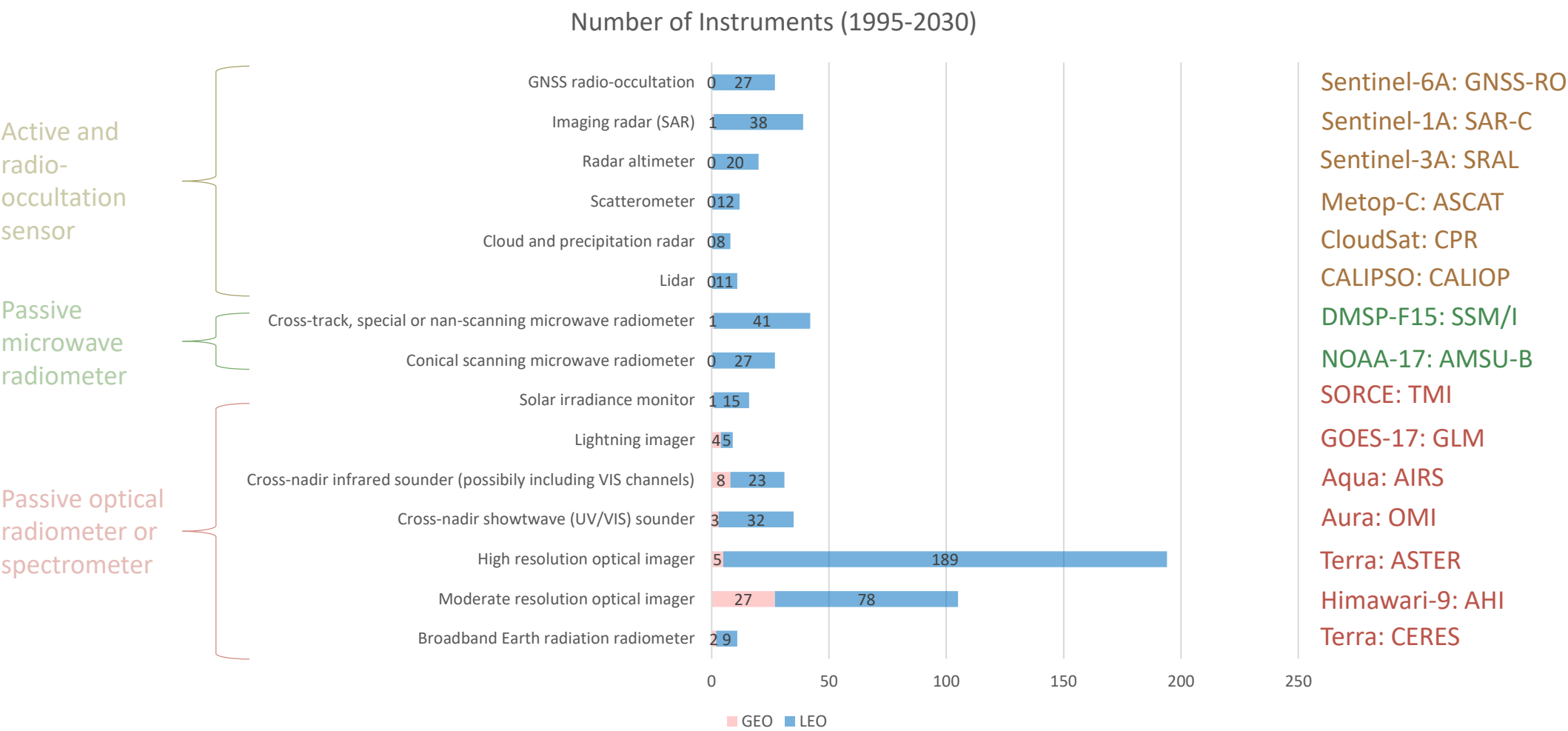


Earth observation instrument types



Data source: OSCAR

Earth observation instrument types (with examples)



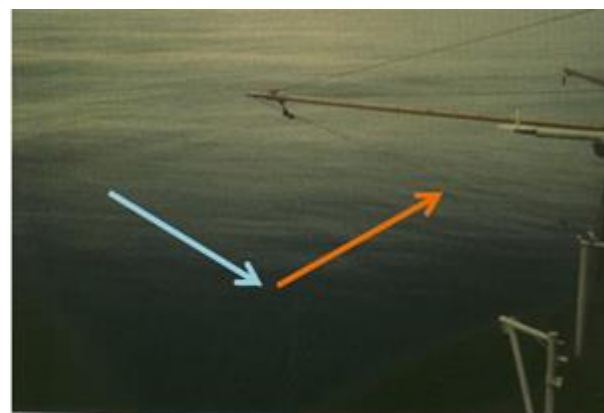
Data source: OSCAR

Scatterometer

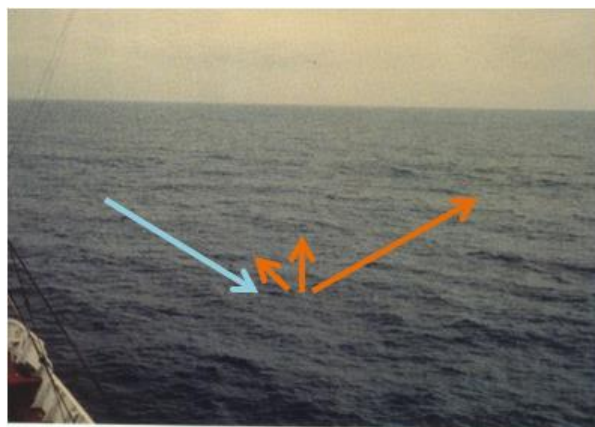
Scatterometers are active remote sensing instruments for deriving wind direction and speed from the roughness of the sea. They transmit electromagnetic pulses and detect the backscattered signals.

Bragg scattering is a scattering mechanism that occurs when electromagnetic radiation and water waves interact with similar wave lengths. The Bragg scattering explains the effects of the reflection of electromagnetic waves on periodic structures whose distances are in the order of the wavelength.

Bragg scattering is dependent on the incident angle. Angles between 30° and 60° are often used to provide the largest sensitivity to changes in wind speed.



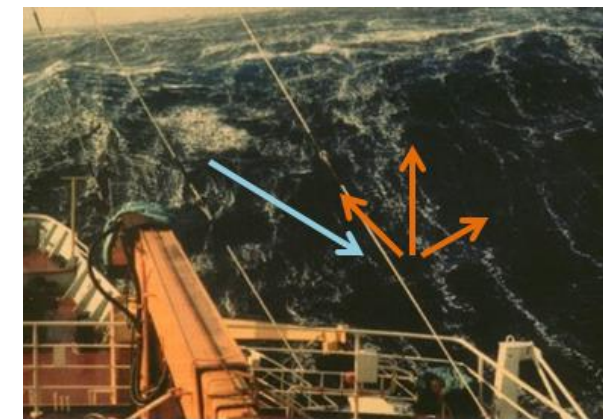
BEAUFORT FORCE 0
WIND SPEED: LESS THAN 1 KNOT
SEA: SEA LIKE A MIRROR



BEAUFORT FORCE 3
WIND SPEED: 7-10 KNOTS
SEA: WAVE HEIGHT 2-3 FT, LARGE WAVELETS,
CRESTS BEGIN TO BREAK, ANY FORM HAS GLASSY
APPEARANCE, SCATTERED WHITE CAPS



BEAUFORT FORCE 6
WIND SPEED: 22-27 KNOTS
SEA: WAVE HEIGHT 9.5-13 FT, LARGER WAVES
BEGIN TO FORM, SPRAY IS PRESENT, WHITE FOAM
CRESTS ARE EVERYWHERE



BEAUFORT FORCE 9
WIND SPEED: 41-47 KNOTS
SEA: WAVE HEIGHT 23-32 FT, HIGH WAVES, DENSE
STREAKS OF FOAM ALONG DIRECTION OF THE WIND,
WAVE CRESTS BEGIN TO TOPPLE, TUMBLE AND
ROLL OVER. SPRAY MAY AFFECT VISIBILITY

Bragg scattering in different Beaufort classes and therefore different states of the sea. Blue arrows show the incoming radar beam, red arrows the scattered radiation. (Credit: EUMETRAIN)

Scatterometer

Scatterometers measure the backscattered signal (radar cross section) by the ripples and waves. A Geophysical Model Function (GMF) is then used to retrieve surface wind from the roughness of the sea.

Given a radar beam with wavelength λ and polarization (ρ), the backscattered and normalized radiation (σ_o) depends on wind vector \mathbf{v} , the relative azimuth angle ϕ between instrument and wind direction, and the incidence angle θ .

$$\sigma_o(\mathbf{v}, \theta, \phi) = \frac{\text{received power}}{\text{transmitted power}}$$

$$\sigma_o(\text{model}) = \text{GMF}(\mathbf{v}, \theta, \phi, \rho, \lambda)$$

A GMF predicts modeled backscatter measurements given a local wind field. In practice, a set of backscatter values is observed, from which the best estimate of the surface wind vector is estimated by minimizing a cost function,

$$\text{MLE}(\mathbf{v}) = \sum_{i=1}^N \left(\frac{z_i^m - z_i^o}{k_p [\sum_{i=1}^N z_i^{o^2}]^{0.5}} \right)$$

where k_p is the normalization factor gives an estimate for the relative accuracy of the observation, given by Stoffelen and Anderson (1997a).

For example, for ASCAT, from triplets of observed backscatter measurements, inversion of a GMF allows for the estimation of the 10-m wind vector.

Scatterometer

Two types of scatterometers – C-band and Ku-band

	C-band	Ku-band
Frequency	5.255 GHz	13.4 GHz
Wavelength	5 cm	2 cm
Limitations	less detection in the higher wind range (> 60 kt), sea ice, coastal coverage - Land contamination	sensitive to rain, coastal coverage - Land contamination
Scatterometer	ASCAT-A and ASCAT-B	QuickScat/RapidSCAT/HY2A
Polarization	VV-pol	Dual-polarization
Sampling	12.5 – 25 km	25 – 50 km
Geometry	Static	Rotating antenna
Swath	Double (about 550 km each)	Single

Scatterometer – short history

C-band Ku-band scatterometer

Skylab (NASA)



1973 (exp)

SEASAT (NASA)



1978 (3 mon)

ERS-1 (ESA)



1991 – 2000

ERS-2 (ESA)



1995 – 2011

ADEOS-1 (NASDA/NASA)



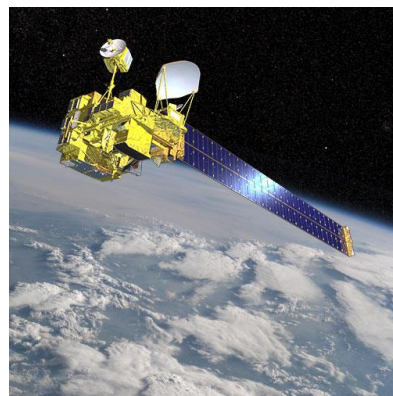
1996 – 1997

Quickscat (NASA)



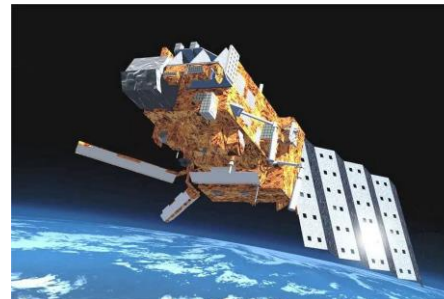
1999 – 2009

ADEOS-2 (NASDA/NASA)



2002 – 2003

METOP-A (EUMETSAT)



2006 – 2021

Oceansat-2 (ISRO)



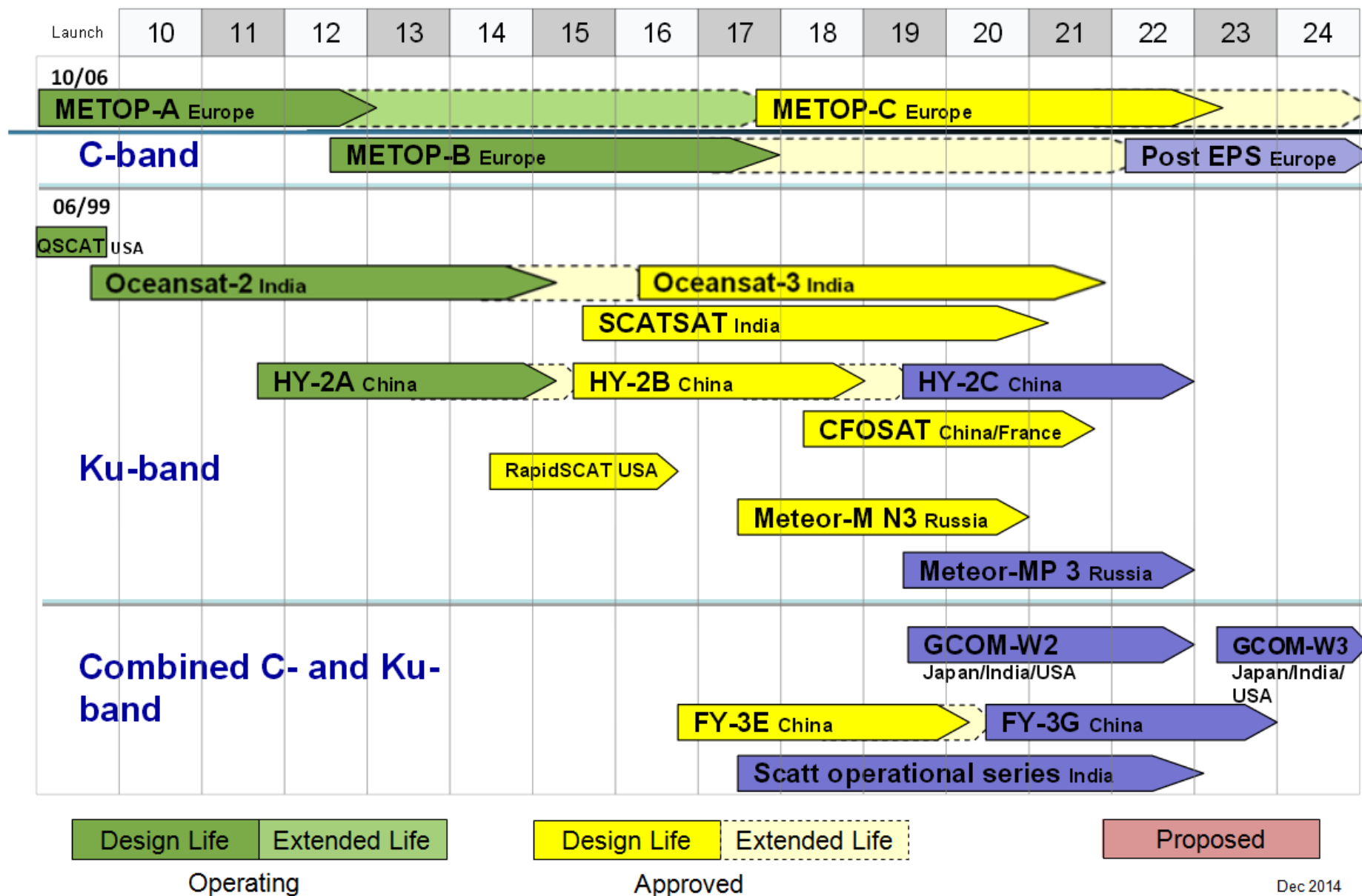
2009 – 2023

METOP-B (EUMETSAT)



2012 – now

Scatterometer – short history (continue)

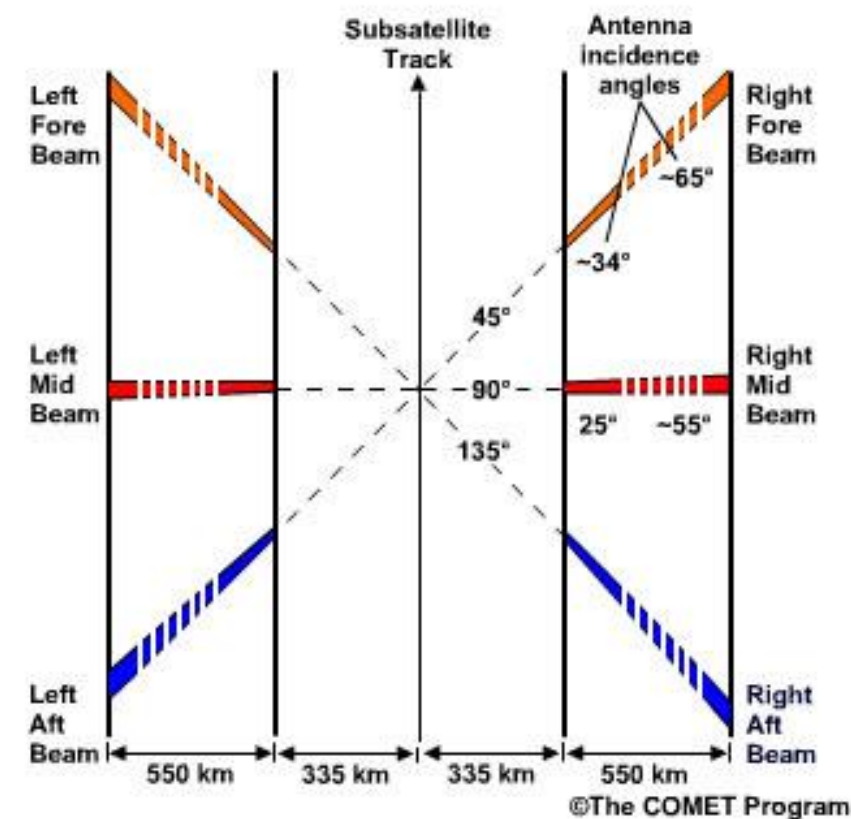
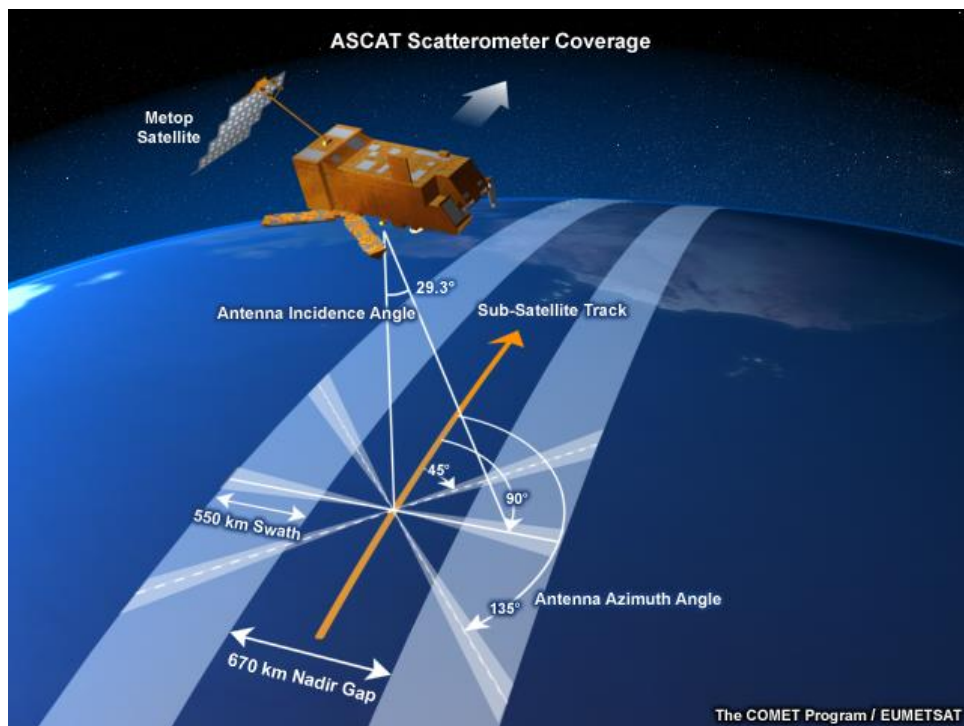


Scatterometer – ASCAT

ASCAT is a **fan beam scatterometer** – a radar with vertically polarized antennas (2 sets x 3). This configuration allows for each point of the surface is seen and measured by the scatterometer three times.

Each beam provides measurements of radar backscatter on a 12.5 km and/or 25 km grid, in such a way that each swath is divided into 41 (41×12.5) or 21 (21×25) so-called Wind Vector Cells (WVCs).

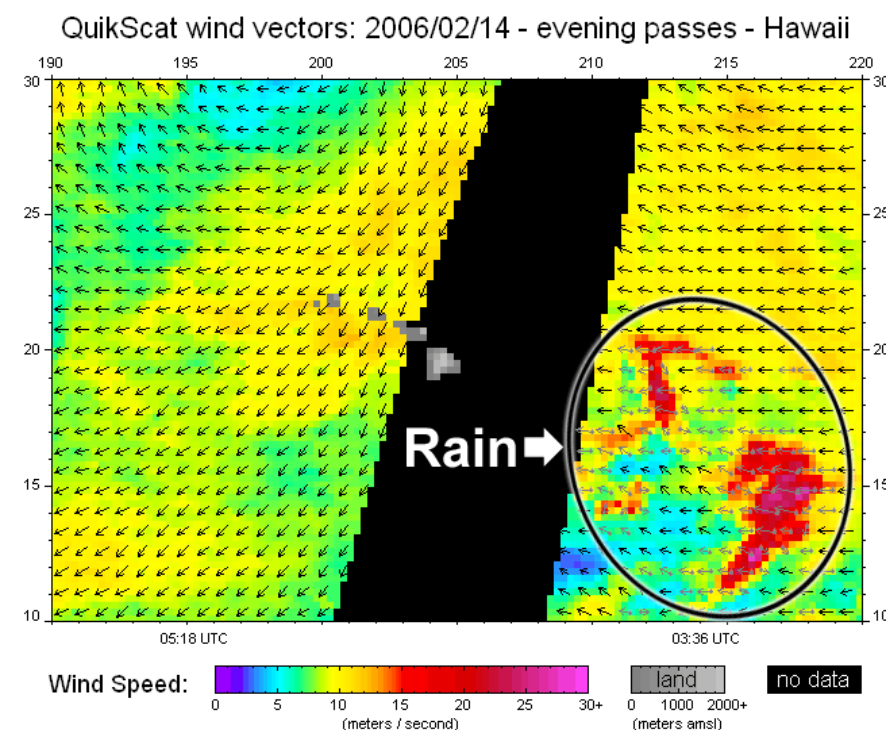
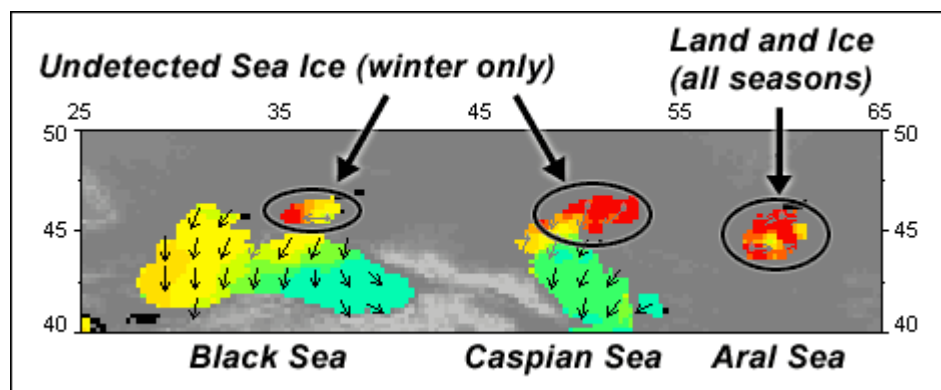
The ASCAT fan beam instrument operates at a frequency of 5.255 GHz (C-band). This makes it generally insensitive to rain, but C-band radars have limitations when it comes to extreme wind speeds larger than 60 knots.



Scatterometer – Limitations

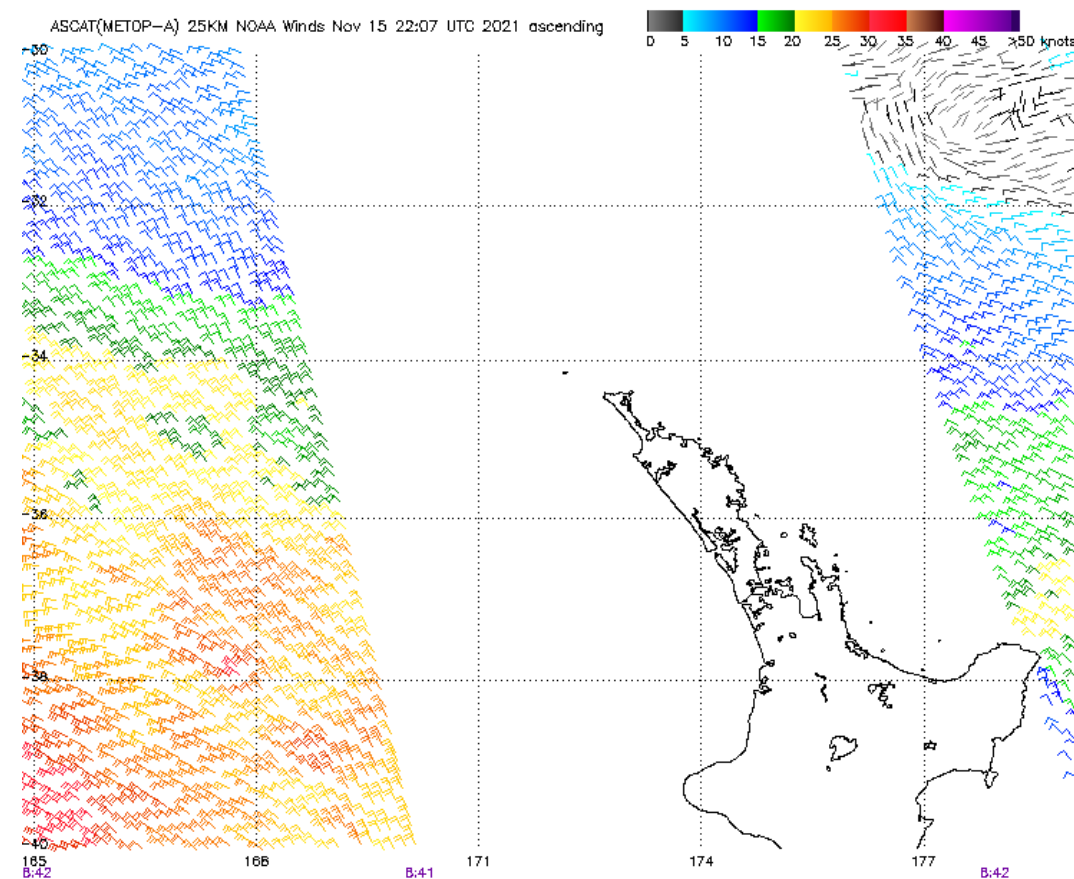
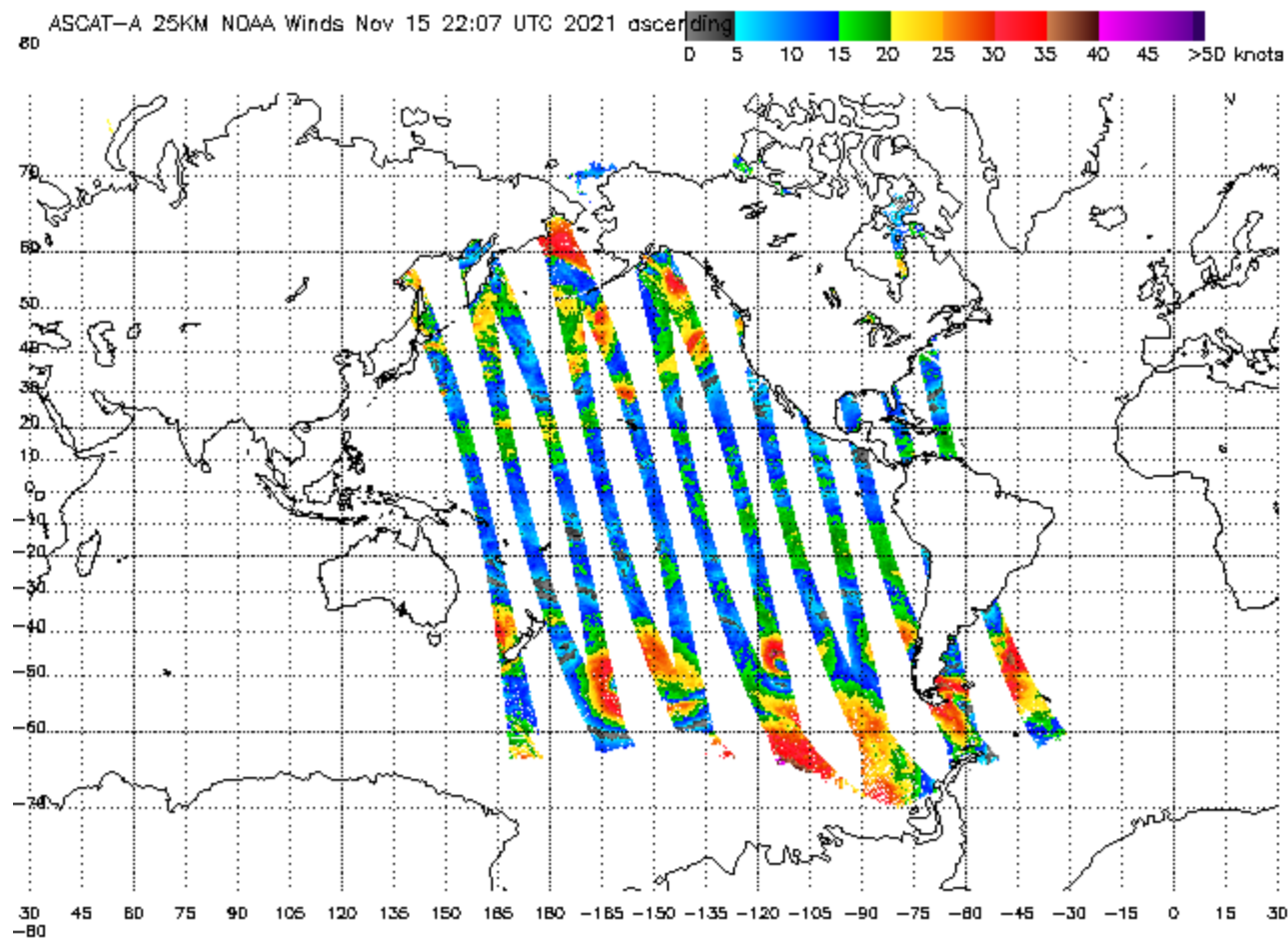
In general, the quality of scatterometer winds is quite good. But there are some situations where the data can be compromised:

- sea ice and land contamination
- large spatial wind variability (for example in the vicinity of fronts and low pressure centers, e.g. downbursts)
- rain - especially in Ku-band systems
- higher wind speeds (>60 knots) - especially in C-band systems



Scatterometer – Product

<https://manati.star.nesdis.noaa.gov/datasets/ASCATData.php>



Note: 1) Times are GMT 2) Times along bottom correspond to measurement at -35S
3) Data buffer is 22 hrs from Nov 15 22:07 UTC 2021 4) Black wind barbs indicate possible contamination
NOAA/NESDIS/Center for Satellite Applications and Research

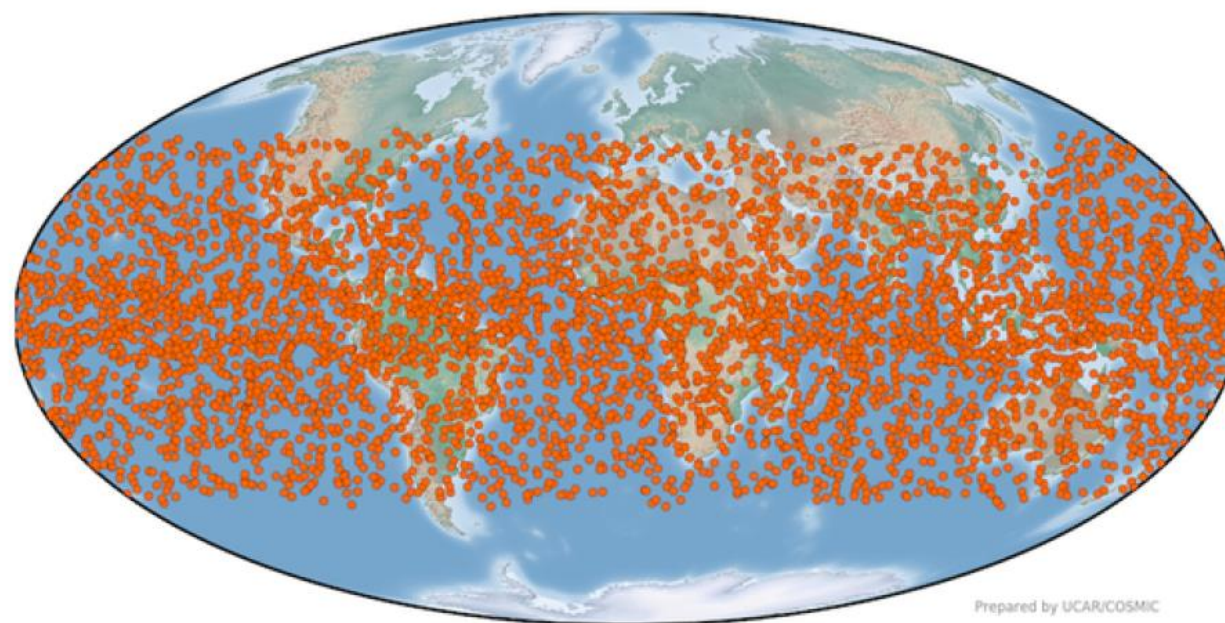
GNSS Radio Occultation

The Global Navigation Satellite System - Radio Occultation is a satellite remote sensing technique that uses GNSS (e.g., GPS) measurements received by a LEO satellite to profile the Earth's atmosphere and ionosphere with high vertical resolution and global coverage.

As radio signals from the GPS satellites (~20,200 km) pass through the atmosphere, molecules and electrons bend their paths and slow their progress. By intercepting the radio signals and measuring their bending and **signal delay** on LEO satellites (~500 km), scientists are able to retrieve profiles of bending angles, refractivity, temperature, pressure, and water vapor in the atmosphere and of electron density in the ionosphere.

Advantages of RO:

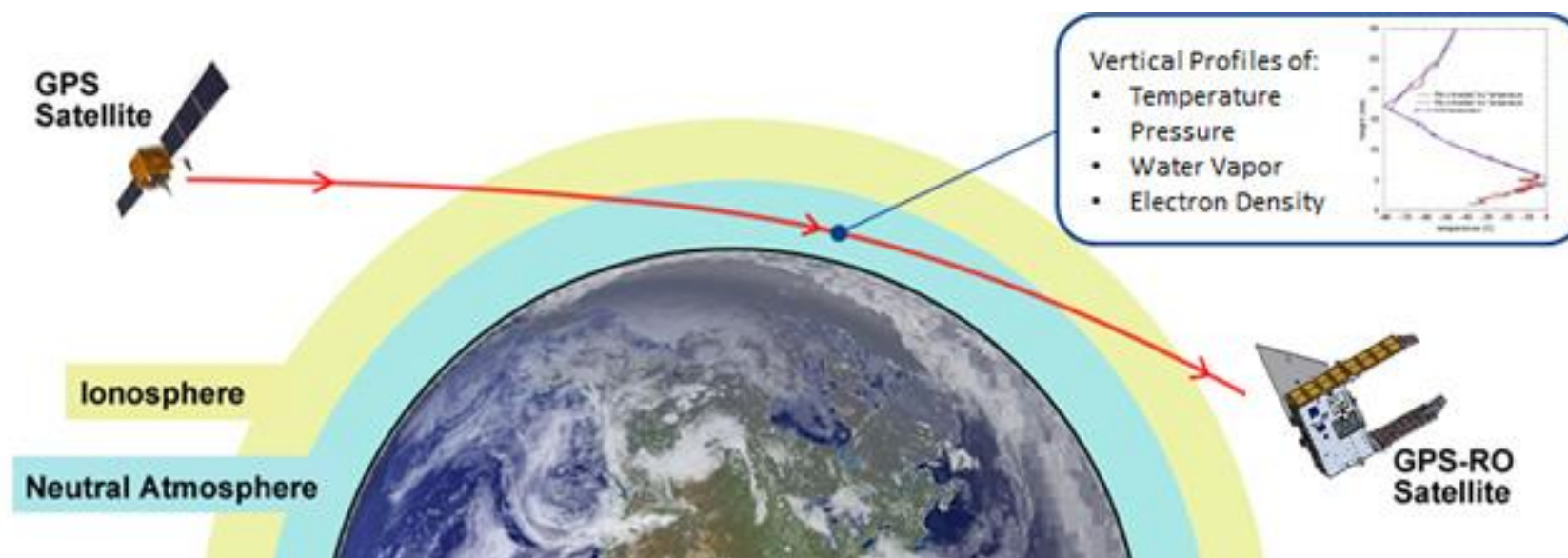
- More accurate forecasts of day-to-day weather
- More accurate hurricane forecasts at longer lead times
- More accurate predictions of heavy-precipitation events
- Improved climate monitoring and research
- Increased data collection over oceans
- Improved space weather forecasts



Geographic coverage provided by COSMIC-2 on October 1, 2019

GNSS Radio Occultation

- RO is an active technique and measurements have been used to study planetary atmospheres (e.g., Mars, Venus) since the 1960's.
- The use of RO measurements in the Earth's atmosphere was originally proposed in 1965, but until 1996, the proof of concept "GPS/MET" experiment demonstrated useful temperature information could be derived from the GPS RO measurements.
- The GPS satellites are primarily a tool for positioning and navigation. These satellites emit radio signals at L1 (1.575 GHz) and L2 (1.227 GHz).
- Because the refractive index is not unity, the GPS signal velocity is modified in the ionosphere and neutral atmosphere. The gradients in the refractive index also "bend" the path.
- The GPS RO is then based on analysing the bending caused the neutral atmosphere along ray paths between a GPS satellite and a receiver placed on a LEO satellite.

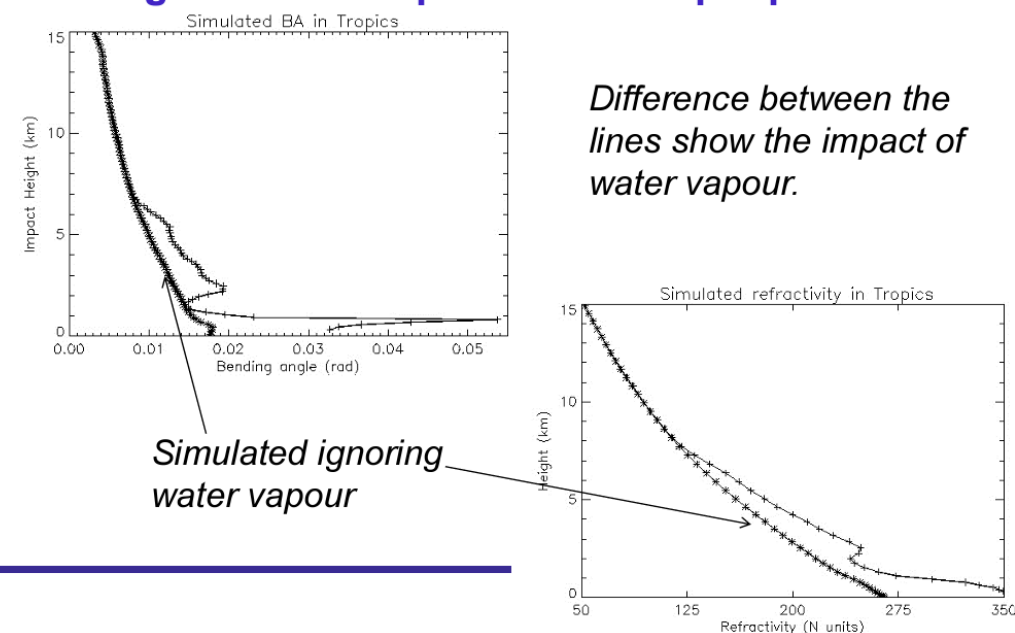


GNSS Radio Occultation

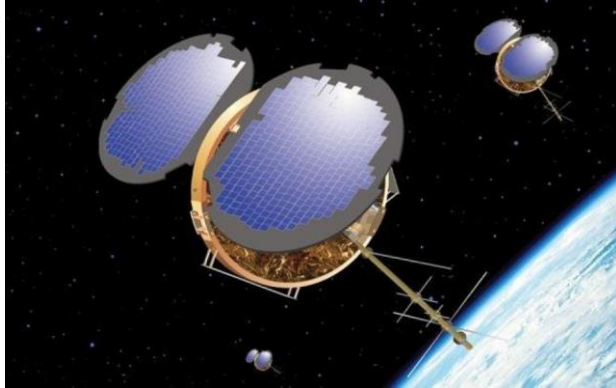
- GPS receivers do not measure bending angle directly.
- Instead, it measures a time series of phase-delays at the two GPS frequencies.
- The accumulated bending angle can be calculated from precise orbit data and the excess phase measurements.
- The bending angle profile can in turn be converted to a refractivity profile using an Abel integration.
- In dry air conditions, atmospheric temperature, pressure, and density profiles can then be retrieved using a refractivity equation, hydrostatic integral, and ideal gas law.
- In moist air conditions, we would expect a T-H ambiguity problem results from moisture's impact on refractivity. Various methods have been proposed to minimize the uncertainty (e.g., Li et al., 2019).

$$N = 77.6 \frac{P}{T} + 3.73 \times 10^5 \frac{e}{T^2}$$

Limitations of classical retrieval: we can't neglect water vapour in the troposphere!



COSMIC-1 (2006 – 2020) and COSMIC-2 (2019 – now)



FORMOSAT-3/COSMIC was launched into a circular low-Earth orbit in 2006 and retired in 2020.

The data from COSMIC-1 have contributed significantly to a wide range of scientific investigation. For example,

1. The data set has led to improved global weather forecasting, especially in data sparse regions including the oceans and near the poles.
2. It has established a global climate change "thermometer" which has unprecedented long-term stability.



The success of COSMIC-1 leads to a follow-on GNSS-RO mission (COSMIC-2) - six COSMIC-2 satellites launched in 2019 into low-inclination orbits.

The main instrument, TGRS (Tri-GNSS Radio-occultation system), was developed by JPL and is tracking more than 4,000 high-quality profiles per day.

With a 24-degree inclination orbit at 720 km altitude, COSMIC-2 occultations primarily distribute from 45 N and 45 S.

GNSS RO data

NOAA NESDIS STAR

GNSS RO Quality Monitor v1.00

NOAA / NESDIS / STAR

ICVS for RO Reload COSMIC-2 COSMIC-1 KOMPSAT-5 Metop CHAMP RadioSonde

Maps

Statistics

Time Series

Profiles

2024 01 15

⏮ ⏪ ⏩ ⏭

Daily

Monthly

Reference

ERA5-f 6h

ERA5-r

GFS 6h

GFS anl

CFS 6h

CFS anl

NCEP-R2

MERRA-2

JRA-55

Interpolation

Height

Pressure

Lat, Lon - starting location of in-situ

Min Alt, Max Alt - valid range of refractivity

UCAR_atmPrf UCAR_wetPrf UCAR_bfrPrf

Showing 1 to 37 of 5,005 entries

Time

Lat

Lon

qf

irs

Leo

GNSS

N Level

T Bias

WV Bias

N Bias

H Bot.

H Top

2024-01-14T23:57:27	15.129	111.094	0	rise	C2E2	g15	2,775				3.18	59.97
2024-01-14T23:57:45	5.476	51.588	0	rise	C2E3	g23	2,877				0.14	59.98
2024-01-14T23:57:45	-25.849	-10.658	0	rise	C2E5	g31	2,888				0.02	59.98
2024-01-14T23:57:58	-13.107	173.595	0	rise	C2E4	r21	2,880				0.00	59.97
2024-01-14T23:58:46	24.641	46.511	0	rise	C2E3	r12	2,853				1.22	59.97
2024-01-14T23:59:34	23.328	51.854	0	rise	C2E3	r02	2,865				0.89	59.96
2024-01-14T23:59:34	-35.073	-179.123	0	rise	C2E4	g30	2,876				0.34	59.96
2024-01-15T00:00:03	-4.255	151.497	0	set	C2E4	g32	2,812				1.98	59.98
2024-01-15T00:00:23	-19.867	-174.902	0	rise	C2E4	g06	2,880				0.01	59.98
2024-01-15T00:00:43	21.280	-164.472	0	set	C2E1	g10	2,894				0.19	59.97
2024-01-15T00:00:51	14.828	61.074	0	rise	C2E3	g25	2,890				0.11	59.96
2024-01-15T00:00:54	-43.394	-5.367	0	rise	C2E5	g18	2,854				1.14	59.97
2024-01-15T00:01:37	-35.032	3.445	0	rise	C2E5	r14	2,847				1.53	59.96
2024-01-15T00:02:23	19.900	-161.433	0	set	C2E1	r13	2,861				1.10	59.96
2024-01-15T00:03:23	-16.861	9.388	0	rise	C2E5	g28	2,892				0.16	59.97
2024-01-15T00:04:20	-35.445	154.395	0	set	C2E4	r17	2,899				0.00	59.97
2024-01-15T00:04:27	-29.694	-34.958	0	set	C2E5	g11	2,883				0.06	59.96
2024-01-15T00:04:37	-4.102	39.026	0	set	C2E3	r16	2,858				0.76	59.97
2024-01-15T00:04:38	29.164	-114.332	0	rise	C2E1	g03	2,872				0.82	59.98
2024-01-15T00:04:41	29.058											
2024-01-15T00:04:59	14.306											
2024-01-15T00:05:21	-18.363											
2024-01-15T00:06:59	-29.134											
2024-01-15T00:08:05	4.318											
2024-01-15T00:09:08	18.031											
2024-01-15T00:09:19	-41.583											
2024-01-15T00:10:01	-3.085											
2024-01-15T00:10:07	38.369											
2024-01-15T00:10:22	1.917											
2024-01-15T00:10:32	6.678											
2024-01-15T00:10:37	22.977											
2024-01-15T00:10:45	29.004											
2024-01-15T00:10:54	-40.434											
2024-01-15T00:10:56	-6.024											
2024-01-15T00:11:09	39.751											
2024-01-15T00:11:20	10.469											
2024-01-15T00:11:25	-27.446											

Platform '2024-01-14T23:57:27_C2E2_g15'

Location

Bending Angle

Refractivity

Temperature

Water Vapor

Pressure

Excess Phase

SNR

2024-01-14T23:57:27 C2E2_g15 UCARdry cosmic2

Platform '2024-01-14T23:57:27_C2E2_g15'

Location Bending Angle Refractivity Temperature Water Vapor Pressure Excess Phase SNR

Bending Angle

Platform '2024-01-14T23:57:27_C2E2_g15'

Location Bending Angle Refractivity Temperature Water Vapor Pressure Excess Phase SNR

Refractivity

Platform '2024-01-14T23:57:27_C2E2_g15'

Location Bending Angle Refractivity Temperature Water Vapor Pressure Excess Phase SNR

Temperature profile (dry air)

Platform '2024-01-14T23:57:27_C2E2_g15'

Location Bending Angle Refractivity Temperature Water Vapor Pressure Excess Phase SNR

Temperature profile

Temperature profile (dry air)

Temperature profile

Platform '2024-01-14T23:57:27_C2E2_g15'

Location Bending Angle Refractivity Temperature Water Vapor Pressure Excess Phase SNR

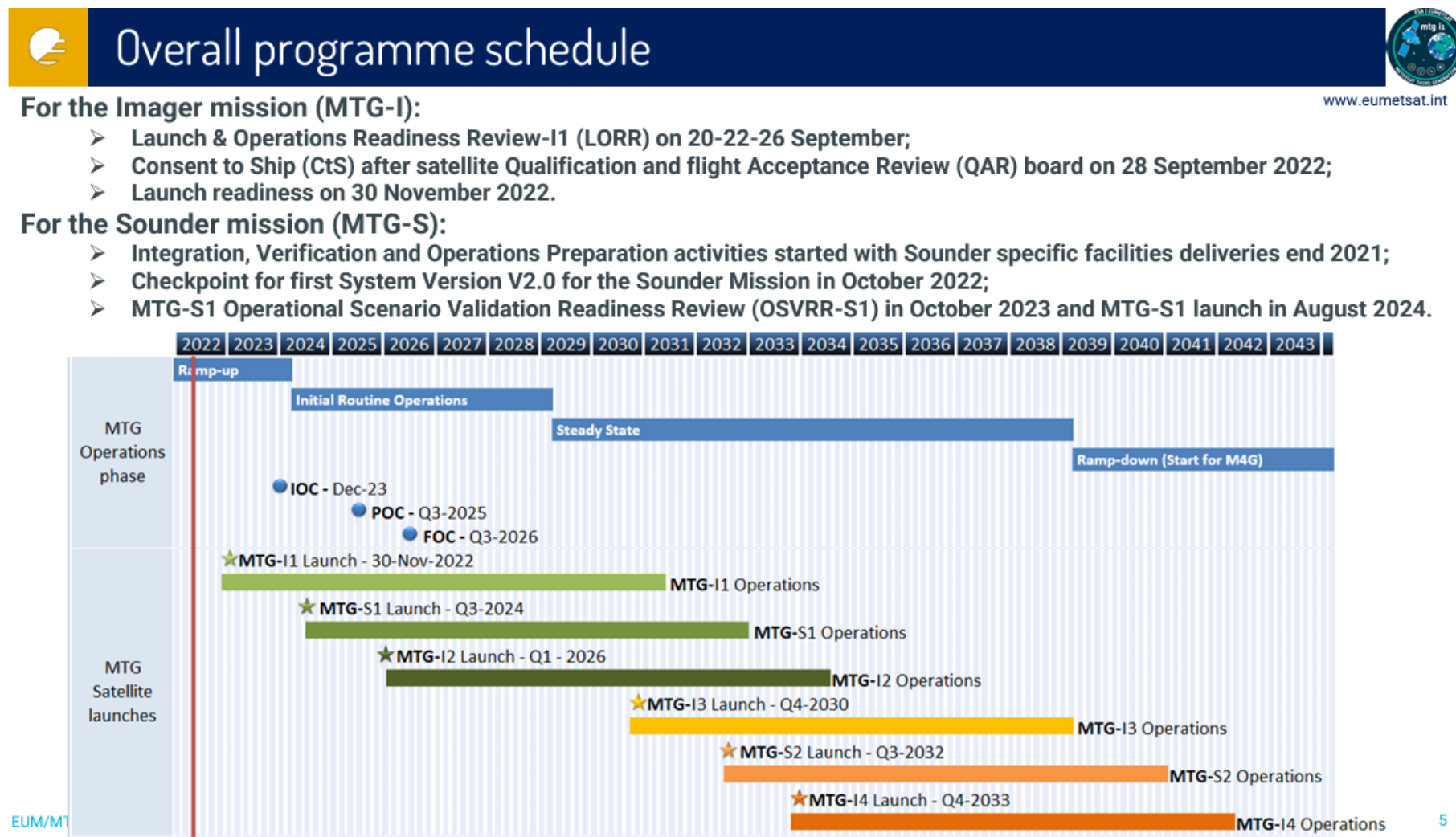
Water Vapor

Illinois at Urbana Champaign

1/28/2024

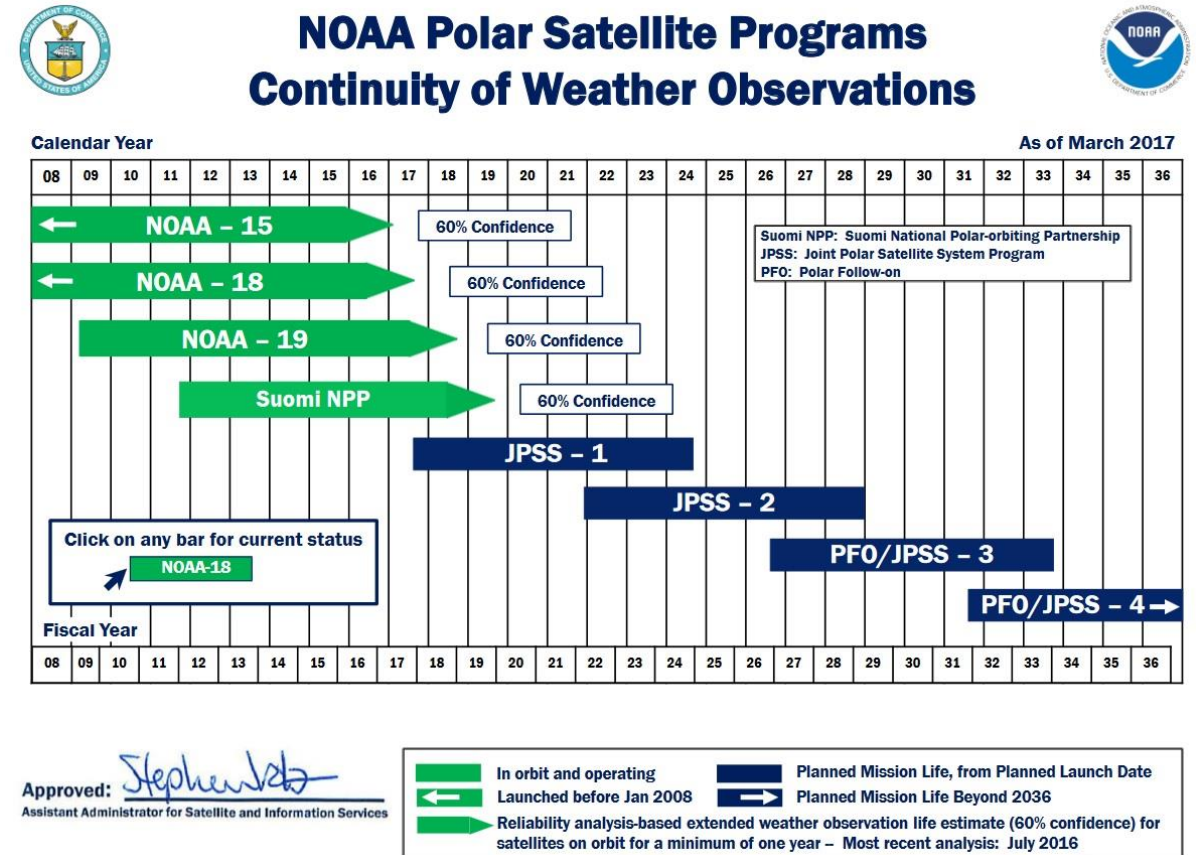
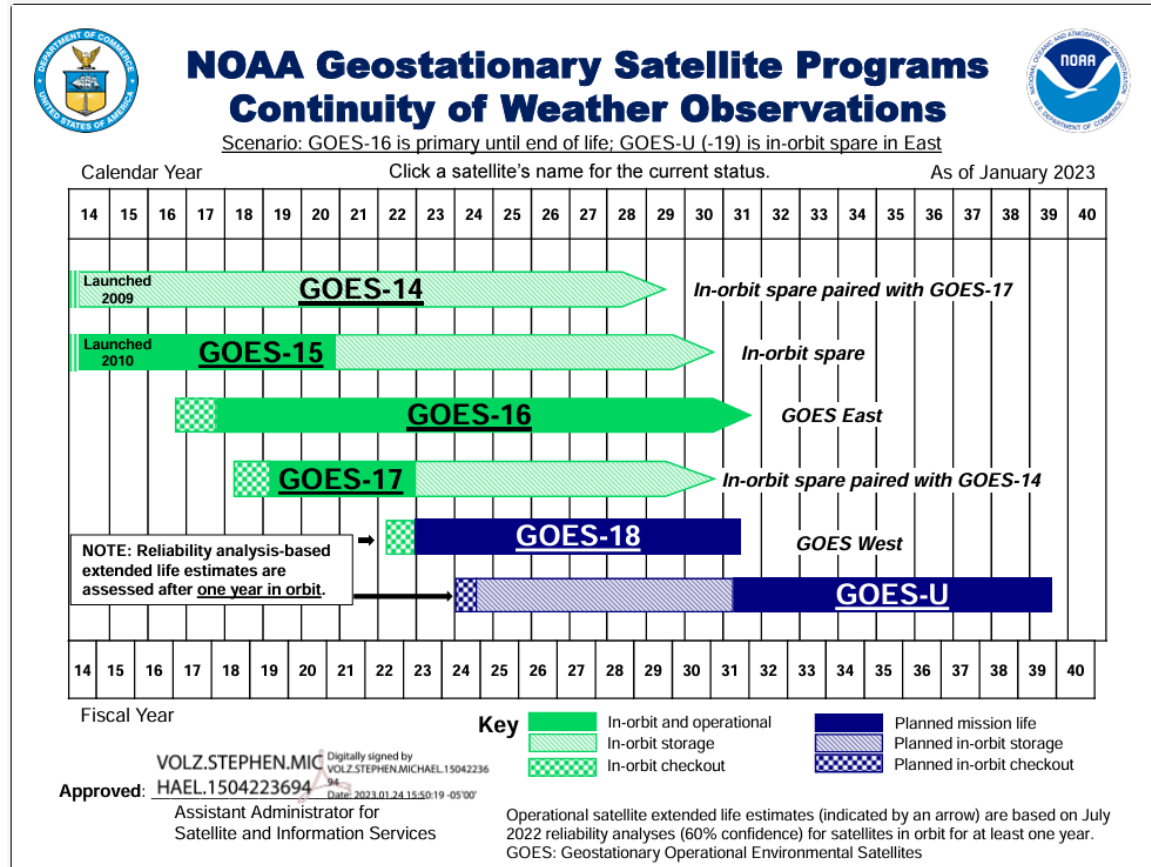
19

EUMETSAT



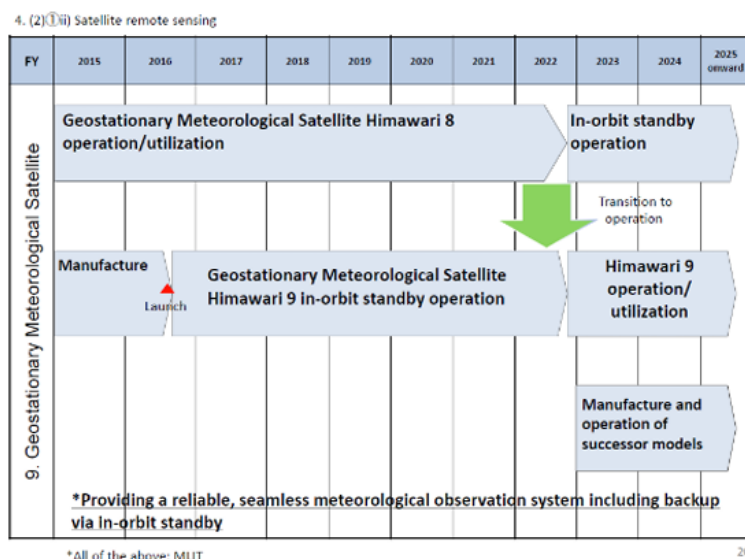
<https://www.eumetsat.int/planned-launches>

NOAA



JMA

- 2018: JMA started considering the next GEO satellite program



[Description of Japan's geostationary meteorological satellites in the Implementation Plan revised in FY2017](#)

The Implementation Plan of the Basic Plan on Space Policy:

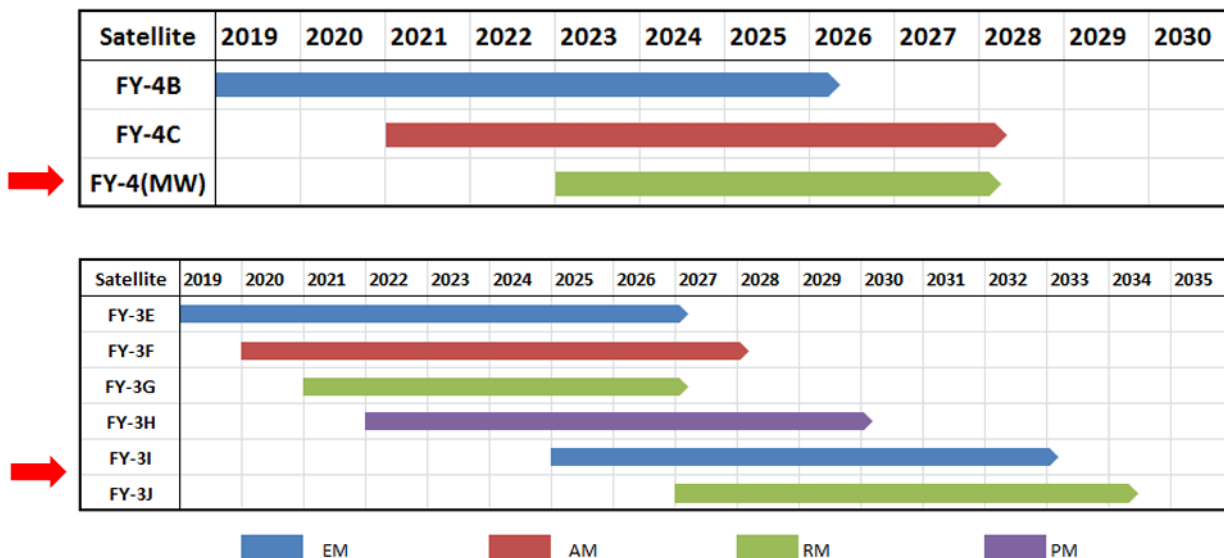
*“By **FY2023** Japan will start manufacturing the Geostationary Meteorological Satellites that will be the successors to Himawari-8 and -9, aiming to **put them into operation in around FY2029**”.*

Vision for WMO Integrated Global Observing System in 2040 for GEO satellites

	Application	Satellite/Instrument
VIS/IR Imager w/ rapid repeat cycles	Cloud amount/type/top height/temperature, wind, sea/land surface temperature, precipitation, aerosols, snow cover, vegetation cover, albedo, atmospheric stability, fires, volcanic ash, sand/dust storm, convective initiation	<ul style="list-style-type: none"> NOAA: GOES-16,17/ABI JMA: Himawari-8,9/AHI KMA: GK-2A/AMI CMA: FY-4A/AGRI EUMETSAT: MTG-I1/FCI (2021)
Hyperspectral IR Sounder	Atmospheric temperature/humidity, wind, rapidly evolving mesoscale features, sea/land surface temperature, cloud amount/top height/temperature, atmospheric composition	<ul style="list-style-type: none"> NOAA: N/A JMA: N/A KMA: N/A CMA: FY-4A/GIIRS EUMETSAT: MTG-S1/IRS (2023)
Lightning Mapper	Lightning, location of intense convection, life cycle of convective systems	<ul style="list-style-type: none"> NOAA: GOES-16,17/GLM JMA: N/A KMA: N/A CMA: FY-4A/LMI EUMETSAT: MTG-I1/LI (2021)
UV/VNIR Sounder	Ozone, trace gases, aerosol, humidity, cloud top height	<ul style="list-style-type: none"> NASA: TEMPO (2022) JMA: N/A KMA: GK-2B/GEMS (2020) CMA: N/A EUMETSAT: MTG-S1/UVN (2023)

CMA

National Space Infrastructure Program for Meteorological Satellites (from 2020 to 2025) approved by the State Council



GIIRS:
First Geo. Interferometric Infrared Sounder

